

~~CONFIDENTIAL~~Copy
RM L50D10

NACA

RESEARCH MEMORANDUM

FLIGHT MEASUREMENTS WITH THE DOUGLAS D-558-II

(BUAERO NO. 37974) RESEARCH AIRPLANE

DETERMINATION OF THE AERODYNAMIC CENTER AND ZERO-LIFT

PITCHING-MOMENT COEFFICIENT OF THE WING-FUSELAGE

COMBINATION BY MEANS OF TAIL-LOAD MEASUREMENTS

IN THE MACH NUMBER RANGE FROM 0.37 TO 0.87

By John P. Mayer, George M. Valentine,
and Geraldine C. MayerLangley Aeronautical Laboratory
Langley Air Force Base, Va.

CLASSIFIED DOCUMENT

This document contains classified information affecting the National Defense of the United States within the meaning of the Espionage Act, USC 50:81 and 82. Its transmission or the revelation of its contents in any manner to an unauthorized person is prohibited by law. Information so classified may be imparted only to persons in the military and naval services of the United States, appropriate civilian officers and employees of the Federal Government who have a legitimate interest therein, and to United States citizens of known loyalty and discretion who of necessity must be informed thereof.

NATIONAL ADVISORY COMMITTEE
FOR AERONAUTICS

WASHINGTON

July 11, 1950

CLASSIFICATION CHANGED

UNCLASSIFIED

To:

By authority of:

Date:

Approved
J.P.M. 10/15/50
R.N. 126
JPM 5-19-58

~~CONFIDENTIAL~~

NATIONAL ADVISORY COMMITTEE FOR AERONAUTICS

RESEARCH MEMORANDUM

FLIGHT MEASUREMENTS WITH THE DOUGLAS D-558-II

(BUAERO NO. 37974) RESEARCH AIRPLANE

DETERMINATION OF THE AERODYNAMIC CENTER AND ZERO-LIFT

PITCHING-MOMENT COEFFICIENT OF THE WING-FUSELAGE

COMBINATION BY MEANS OF TAIL-LOAD MEASUREMENTS

IN THE MACH NUMBER RANGE FROM 0.37 TO 0.87

By John P. Mayer, George M. Valentine,
and Geraldine C. Mayer


SUMMARY

Flight measurements of aerodynamic tail loads have been made on the Douglas D-558-II airplane from which the variation with Mach number of the wing-fuselage aerodynamic center, the static-longitudinal-stability parameter $(\partial C_M / \partial C_L)_{WF}$, the tail load per g, and the zero-lift wing-

fuselage pitching-moment coefficient have been determined up to a Mach number of 0.87. These measurements indicate that for the normal-force-coefficient range covered in these tests the wing-fuselage aerodynamic center moves rearward with Mach number up to a Mach number of 0.87. The wing-fuselage aerodynamic center is about 10 percent of the mean aerodynamic chord at a Mach number of 0.37 and moves gradually rearward to 15 percent of the mean aerodynamic chord at a Mach number of 0.80. From a Mach number of 0.80 to 0.87 the aerodynamic center moves more rapidly rearward to about 20 percent of the mean aerodynamic chord.

The wing-fuselage pitching-moment coefficient at zero lift $(C_{M_0})_{WF}$ is approximately -0.04 and does not vary with Mach number up to a Mach number of 0.87.

The aerodynamic horizontal-tail load per g found from these measurements for the Douglas D-558-II airplane for a weight of 9600 pounds and a center-of-gravity location of 26 percent mean aerodynamic chord is



about 520 pounds per g at a Mach number of 0.37 and decreases to about 400 pounds per g at a Mach number of 0.80. As the Mach number increases from 0.80 to 0.87 the tail load per g decreases to about 200 pounds per g.

INTRODUCTION

As a portion of the cooperative NACA-Navy Transonic Flight Research Program, the NACA is utilizing the Douglas D-558-II research airplane. These tests are being made at the NACA High-Speed Flight Research Station at Edwards Air Force Base, Calif. This paper presents results from the measurements of the horizontal-tail loads by means of strain gages in the Mach number range from 0.37 to 0.87. From these measurements the variation with Mach number of the wing-fuselage aerodynamic center, the static-longitudinal-stability parameter $(\partial C_M / \partial C_L)_{WF}$, the zero-lift wing-fuselage pitching-moment coefficient $(C_{M_0})_{WF}$, and the tail load per g were found and are presented in this paper.

The Douglas D-558-II airplane is longitudinally unstable at high normal-force coefficients. The values of the aerodynamic center $(\partial C_M / \partial C_L)_{WF}$ and the tail load per g presented in this paper were determined in the normal-force-coefficient range for which the airplane is longitudinally stable.

Results on other aerodynamic characteristics of the Douglas D-558-II airplane have been presented in references 1 and 2.

SYMBOLS

$(a.c.)_{WF}$	aerodynamic center of wing-fuselage combination, percent mean aerodynamic chord
\bar{c}	mean aerodynamic chord (M.A.C.), feet
c.g.	airplane center of gravity, percent mean aerodynamic chord
C_{N_A}	airplane normal-force coefficient (Normal force/ qS_W)
C_{N_T}	tail normal-force coefficient (L_T/qS_T)
$C_{N_{T_C}}$	tail normal-force coefficient, corrected for pitching acceleration (L_{T_C}/qS_T)

$(C_{M_0})_{WF}$	wing-fuselage zero-lift pitching-moment coefficient ($M_0/qS_w\bar{c}$)
$(\partial C_M/\partial C_L)_{WF}$	static-longitudinal-stability parameter (x/\bar{c})
g	acceleration of gravity, feet per second per second
I_y	airplane moment of inertia in pitch, slug-feet square $\left(\frac{W}{g} K_y^2\right)$
K_y	radius of gyration in pitch (approx. 9.6 ft), feet
l_T	tail length (measured between the airplane center of gravity and the intersection of the 0.30 chord line and the midsemispan of the horizontal tail; $l_T = 19.9$ ft for c.g. = 26 percent M.A.C.), feet
L_T	total aerodynamic horizontal-tail load (up tail load positive), pounds
L_{Tc}	total aerodynamic horizontal-tail load corrected for pitching acceleration, pounds
M	free-stream Mach number
M_0	zero-lift wing-fuselage pitching moment, foot-pounds
n_A	airplane normal-load factor, g units
q	dynamic pressure, pounds per square foot $\left(\frac{1}{2}\rho V^2\right)$
q_1	dynamic pressure at start of any maneuver, pounds per square foot
S_w	wing area, square feet
S_T	horizontal-tail area, square feet
W	airplane gross weight, pounds
W_S	standard airplane gross weight (9600 lb), pounds
x	distance from aerodynamic center of wing-fuselage combination to airplane center of gravity (positive if (a.c.) _{WF} is forward of c.g.), feet

ρ mass density of air, slugs per cubic foot
 $\ddot{\theta}$ pitching acceleration, radians per second per second

AIRPLANE

The Douglas D-558-II airplane has sweptback wing and tail surfaces and was designed for combination turbojet and rocket power plant. The airplane being used in the present investigation (BuAero No. 37974) does not yet have the rocket engine installed. This airplane is powered only by a J-34-WE-40 turbojet engine which exhausts out of the bottom of the fuselage between the wing and the tail. Both slats and stall-control vanes are incorporated on the wing of the airplane. The wing slats can be locked in the closed position or they can be unlocked. When the slats are unlocked, the slat position is a function of the angle of attack of the airplane. The airplane is equipped with an adjustable stabilizer. Photographs of the airplane are shown in figures 1 and 2 and a three-view drawing is shown in figure 3. A drawing of the wing section showing the wing slat in the closed and extended positions is given in figure 4. Pertinent airplane dimensions and characteristics are listed in table I.

INSTRUMENTATION AND ACCURACY

Standard NACA recording instruments are installed in the airplane to measure the following quantities:

- Airspeed
- Altitude
- Elevator and aileron wheel force
- Rudder-pedal force
- Normal, longitudinal, and transverse acceleration at the center of gravity of the airplane
- Normal, longitudinal, and transverse accelerations at the tail
- Pitching, rolling, and yawing velocities
- Airplane angle of attack
- Stabilizer, elevator, rudder, aileron, and slat positions

Strain gages are installed on the airplane structure to measure wing and tail loads. A schematic drawing showing the horizontal-tail gage locations is given in figure 5. The strain-gage circuits operate on direct current. The outputs of the strain gages were recorded on an 18-channel recording oscillograph. The strain gages were calibrated in terms of tail load by applying known loads at many points on the tail

structure. The measured outputs of the gages were utilized to obtain equations from which the load on the tail could be found from the gage responses during flight. In flight, the strain gages respond to a combination of aerodynamic and inertia loads. The loads given in this paper have been corrected for inertia effects and represent aerodynamic loadings.

A free-swiveling-airspeed head was used to measure both static and total pressures. This airspeed head was mounted on a boom approximately 7 feet forward of the nose of the airplane. The vane which was used to measure angle of attack was mounted below the same boom approximately $4\frac{1}{2}$ feet forward of the nose of the airplane.

The airspeed system was calibrated for position error up to a Mach number of 0.70 by making tower passes. The swiveling airspeed head used on the airplane was calibrated in a wind tunnel for instrument error up to a Mach number of 0.85. Tests of similar nose-boom installations indicate that the position error due to the flow field of the fuselage does not vary with Mach number up to a Mach number of 0.90.

The estimated accuracies of the measured quantities pertinent to this paper are as follows:

M	±0.01
L_T , pounds	±50
n_A , g	±0.02

RESULTS AND DISCUSSION

All the data presented were obtained with power on and the airplane in the clean condition, gear and flaps up. Data are presented for both slats-locked-closed and slats-unlocked configurations. The data presented herein were obtained in the left and right turns at altitudes from about 10,000 feet to 25,000 feet and in the normal-force coefficient and Mach number ranges shown in figure 6.

Typical data are presented in time-history form and as plots of tail loads against load factor and tail normal-force coefficient against airplane normal-force coefficient.

The horizontal-tail load may be given as

$$L_T = n_A W \frac{\frac{x}{c}}{\frac{x}{c} + \frac{l_T}{c}} + (C_{M_O})_{WF} \frac{q \frac{S_w}{c}}{\frac{x}{c} + \frac{l_T}{c}} - \frac{I_y \ddot{\theta}}{x + l_T} \quad (1)$$

and the tail normal-force coefficient based on the free-stream dynamic pressure is

$$C_{N_T} = C_{N_A} \frac{S_w}{S_T} \frac{\frac{x}{\bar{c}}}{\frac{x}{\bar{c}} + \frac{l_T}{\bar{c}}} + \frac{(C_{M_O})_{WF} \left(\frac{S_w}{S_T} \right)}{\frac{x}{\bar{c}} + \frac{l_T}{\bar{c}}} - \frac{I_y \ddot{\theta}}{(x + l_T) q S_T} \quad (2)$$

Then, in order to account for changes in weight and changes in dynamic pressure during any maneuver, the tail load may be given as

$$L_{T_C} \frac{W_S}{W} \frac{q_1}{q} = \frac{n_A q_1}{q} \frac{W_S \frac{x}{\bar{c}}}{\frac{x}{\bar{c}} + \frac{l_T}{\bar{c}}} + (C_{M_O})_{WF} \frac{q_1 S_w}{\frac{x}{\bar{c}} + \frac{l_T}{\bar{c}}} \frac{W_S}{W} \quad (3)$$

where L_{T_C} is defined as

$$L_{T_C} = L_T + \frac{I_y \ddot{\theta}}{x + l_T} \quad (4)$$

and where W_S is an arbitrary standard weight taken as 9600 pounds and q_1 is the dynamic pressure at the beginning of any one maneuver.

From these equations the static-longitudinal-stability parameter $(\partial C_M / \partial C_L)_{WF}$, the wing-fuselage aerodynamic center, the tail load per g (dL_T / dn_A) , and the zero-lift wing-fuselage pitching-moment coefficient $(C_{M_O})_{WF}$ can be determined.

$$\left(\frac{\partial C_M}{\partial C_L} \right)_{WF} = \frac{x}{\bar{c}} \quad (5)$$

$$\frac{x}{c} = \frac{\frac{L_T}{c} \frac{dL_{TC}}{dn_A} \frac{W_S}{W} \frac{q_1}{q}}{\left(W_S - \frac{dL_{TC}}{dn_A} \frac{W_S}{W} \frac{q_1}{q} \right)} \quad (6)$$

$$(a.c.)_{WF} = c.g. - \frac{x}{c} \quad (7)$$

$$\frac{dL_T}{dn_A} = \frac{W \frac{x}{c}}{\frac{x}{c} + \frac{L_T}{q}} \quad (8)$$

From the values obtained for x/c , $(C_{M_O})_{WF}$ may be determined from equation (3).

A time history of the measured quantities during a turn is shown in figure 7. The variation of $L_{TC} \frac{W_S}{W} \frac{q_1}{q}$ with $n_A \frac{q_1}{q}$ and the horizontal-tail normal-force coefficient with airplane normal-force coefficient for this maneuver are shown in figures 8 and 9, respectively. The values of aerodynamic center, $(\partial C_M / \partial C_L)_{WF}$, tail load per g, and $(C_{M_O})_{WF}$ presented in this paper were obtained from data such as those shown in figures 7 to 9. The wind-tunnel tests of reference 3 indicate that the wing-fuselage aerodynamic center varies somewhat with lift coefficient. The data obtained from the present flight tests indicate that the movement of the aerodynamic center with normal-force coefficient is small for the Mach number and normal-force-coefficient range presented in this paper.

The variation of the wing-fuselage aerodynamic center with Mach number is shown in figure 10. At a Mach number of 0.37 the aerodynamic center is located at 10 percent of the mean aerodynamic chord and moves gradually rearward to 15 percent of the mean aerodynamic chord at a Mach

number of 0.80. From a Mach number of 0.80 to 0.87 the aerodynamic center moves rearward fairly abruptly to about 20 percent of the mean aerodynamic chord.

Also shown in figure 10 is the variation of the aerodynamic center with Mach number for the Douglas D-558-II airplane obtained in the wind-tunnel tests of reference 3. The flight tests indicate that the aerodynamic center is approximately 4 percent of the mean aerodynamic chord farther forward than indicated in the wind-tunnel tests. A part of this difference may be attributed to the difference in configurations. The wind-tunnel model did not have intake ducts and had a flush-type canopy.

The abrupt movement of the wing-fuselage aerodynamic center to the rear, shown beyond a Mach number of 0.80, was indicated in the flight tests for airplane normal-force coefficients below 0.4. The wind-tunnel data indicate a similar trend at comparable lift coefficients.

The variation of the static-longitudinal-stability parameter $(\partial C_M / \partial C_L)_{WF}$ with Mach number is shown in figure 11. The data are presented for a center-of-gravity position of 26 percent of the mean aerodynamic chord. Also shown are the wind-tunnel data of reference 3 corrected to the same center-of-gravity location. These data indicate a gradual increase in stability of the wing-fuselage combination between a Mach number of 0.37 and 0.80, and a more abrupt increase in stability at Mach numbers between 0.80 and 0.87.

An application of the preceding results is shown in figure 12 as the variation of the horizontal-tail load per g dL_T/dn with Mach number. Data are presented for a center-of-gravity location of 26 percent of the mean aerodynamic chord and a weight of 9600 pounds. These data indicate that the tail load per g decreases from 520 pounds per g at a Mach number of 0.37 to 400 pounds per g at a Mach number of 0.80. From a Mach number of 0.80 to 0.87 the tail load per g decreases to approximately 200 pounds per g.

The variation of the pitching-moment coefficient of the wing-fuselage combination at zero airplane lift $(C_{M_0})_{WF}$ with Mach number is shown in figure 13. Also shown are the results from the wind-tunnel tests of reference 3. There is no appreciable change in $(C_{M_0})_{WF}$ for Mach numbers up to 0.87 and the data are in general agreement with the wind-tunnel data. The value of $(C_{M_0})_{WF}$ obtained from the flight tests is about -0.04.

SUMMARY OF RESULTS

Flight measurements of aerodynamic tail loads on the Douglas D-558-II research airplane at Mach numbers up to 0.87 have indicated the following results:

1. For the normal-force-coefficient range covered in these tests, the wing-fuselage aerodynamic center moves gradually rearward with Mach numbers from 10 percent of the mean aerodynamic chord at a Mach number of 0.37 to 15 percent of the mean aerodynamic chord at a Mach number of 0.80 indicating a gradual increase in the stability of the wing-fuselage combination. From a Mach number of 0.80 to 0.87 the aerodynamic center moves more abruptly rearward to about 20 percent of the mean aerodynamic chord.

2. The wing-fuselage pitching-moment coefficient at zero lift $(C_{M_0})_{WF}$ is approximately -0.04 and does not vary with Mach number up to a Mach number of 0.87.

3. The aerodynamic horizontal-tail load per g is 520 pounds per g at a Mach number of 0.37 and decreases to 400 pounds per g at a Mach number of 0.80. As the Mach number increases from 0.80 to 0.87 the tail load per g decreases to about 200 pounds per g.

Langley Aeronautical Laboratory
National Advisory Committee for Aeronautics
Langley Air Force Base, Va.

REFERENCES

1. Sjoberg, S. A.: Flight Measurements with the Douglas D-558-II (BuAero No. 37974) Research Airplane. Static Lateral and Directional Stability Characteristics as Measured in Sideslips at Mach Numbers up to 0.87. NACA RM L50C14, 1950.
2. Mayer, John P., and Valentine, George M.: Flight Measurements with the Douglas D-558-II (BuAero No. 37974) Research Airplane. Measurements of the Buffet Boundary and Peak Airplane Normal-Force Coefficients at Mach Numbers up to 0.90. NACA RM L50E31, 1950.
3. Osborne, Robert S.: High-Speed Wind-Tunnel Investigation of the Longitudinal Stability and Control Characteristics of a $\frac{1}{16}$ -Scale Model of the D-558-2 Research Airplane at High Subsonic Mach Numbers and a Mach Number of 1.2. NACA RM L9C04, 1949.

TABLE I

DIMENSIONS AND CHARACTERISTICS OF THE
DOUGLAS D-558-II AIRPLANE

Wing:

Root airfoil section (normal to 0.30 chord)	NACA 63-010
Tip airfoil section (normal to 0.30 chord)	NACA 63-012
Total area, sq ft	175.0
Span, ft	25.0
Mean aerodynamic chord, in.	87.301
Root chord (parallel to plane of symmetry), in.	108.508
Tip chord (parallel to plane of symmetry), in.	61.180
Taper ratio	0.565
Aspect ratio	3.570
Sweep at 0.30 chord, deg	35.0
Incidence at fuselage center line, deg	3.0
Dihedral, deg	-3.0
Geometric twist, deg	0
Total aileron area (aft of hinge), sq ft	9.8
Aileron travel (each), deg	±15
Total flap area, sq ft	12.58
Flap travel, deg	50

Horizontal tail:

Root airfoil section (normal to 0.30 chord)	NACA 63-010
Tip airfoil section (normal to 0.30 chord)	NACA 63-010
Area (including fuselage), sq ft	39.9
Span, in.	143.6
Mean aerodynamic chord, in.	41.75
Root chord (parallel to plane of symmetry), in.	53.6
Tip chord (parallel to plane of symmetry), in.	26.8
Taper ratio	0.50
Aspect ratio	3.59
Sweep at 0.30 chord line, deg	40.0
Dihedral, deg	0
Elevator area, sq ft	9.4
Elevator travel, deg	25 up, 15 down
Stabilizer travel, deg	4 L.E. up, 5 L.E. down


 NACA

TABLE I
DIMENSIONS AND CHARACTERISTICS OF THE
DOUGLAS D-558-II AIRPLANE - Concluded

Vertical tail:

Airfoil section (parallel to fuselage center line) . . .	NACA 63-010
Area, sq ft	36.6
Height from fuselage center line, in.	98.0
Root chord (parallel to fuselage center line), in.	146.0
Tip chord (parallel to fuselage center line), in.	44.0
Sweep angle at 0.30 chord, deg	49.0
Rudder area (rearward of hinge line), sq ft	6.15
Rudder travel, deg	±25

Fuselage:

Length, ft	42.0
Maximum diameter, in.	60.0
Fineness ratio	8.40
Speed-retarder area, sq ft	5.25

Power plant J-34-WE-40
two jets for take-off

Airplane weight (full fuel), lb 10,645

Airplane weight (no fuel), lb 9,085

Airplane weight (full fuel and two jets), lb 11,060

Center-of-gravity locations:

Full fuel (gear down), percent mean aerodynamic chord	25.3
Full fuel (gear up), percent mean aerodynamic chord	25.8
No fuel (gear down), percent mean aerodynamic chord	26.8
No fuel (gear up), percent mean aerodynamic chord	27.5
Full fuel and two jets (gear down), percent mean aerodynamic chord	29.2



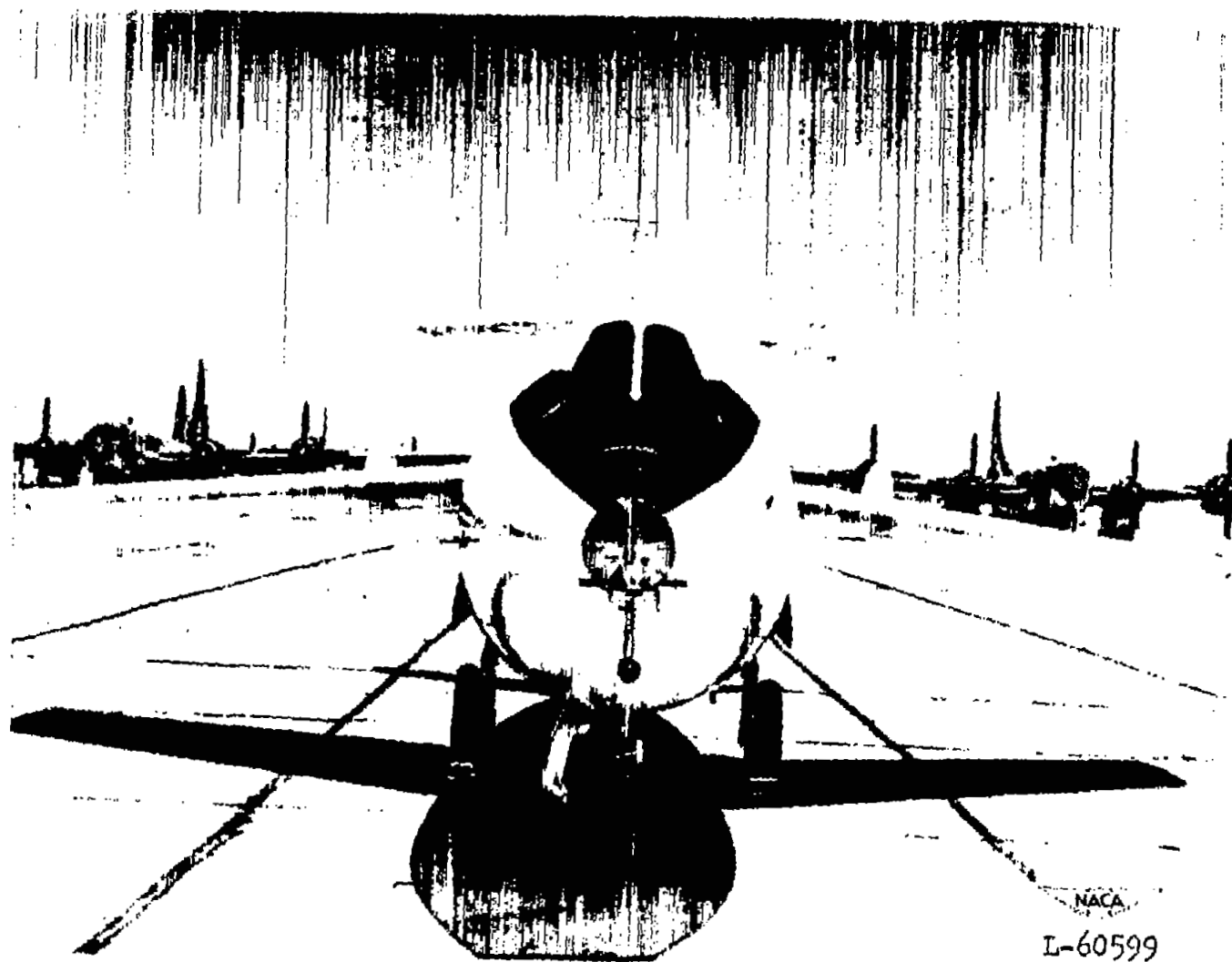


Figure 1.- Front view of Douglas D-558-II (BuAero No. 37974) research airplane.

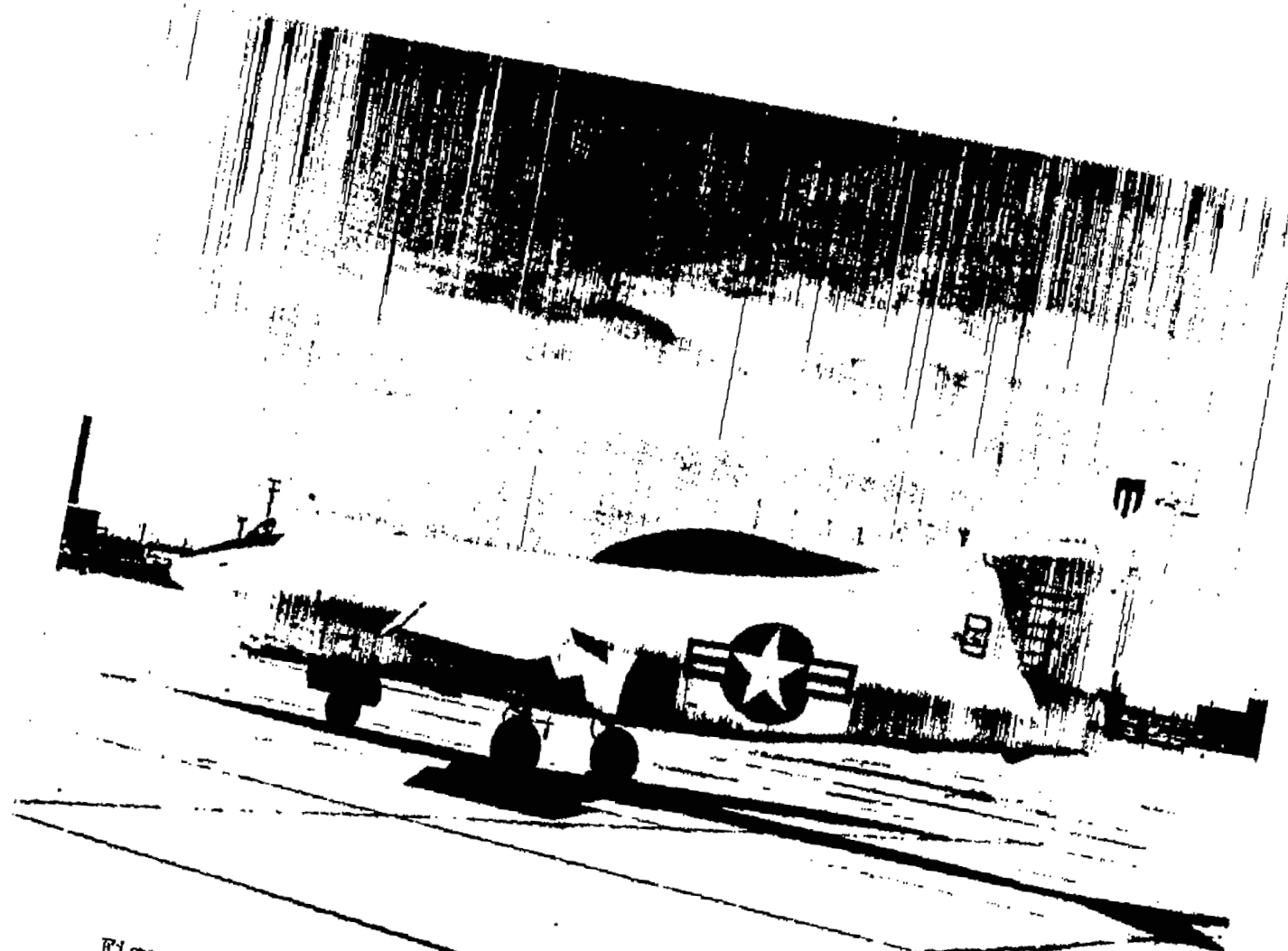


Figure 2.- Three-quarter rear view of Douglas D-558-II (BuAero No. 37974) research airplane.

NACA
L-60600

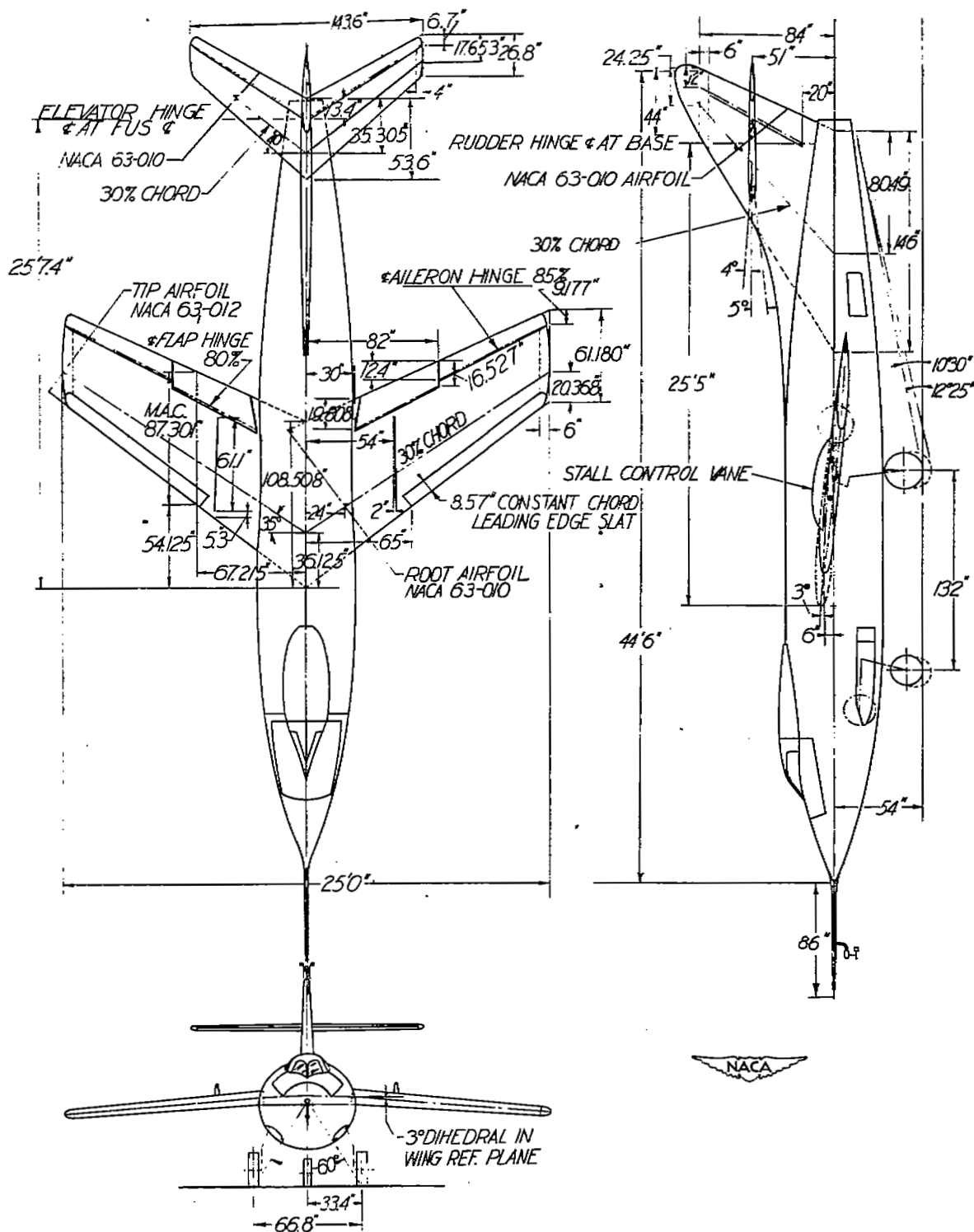


Figure 3.- Three-view drawing of the Douglas D-558-II (BuAero No. 37974) research airplane.

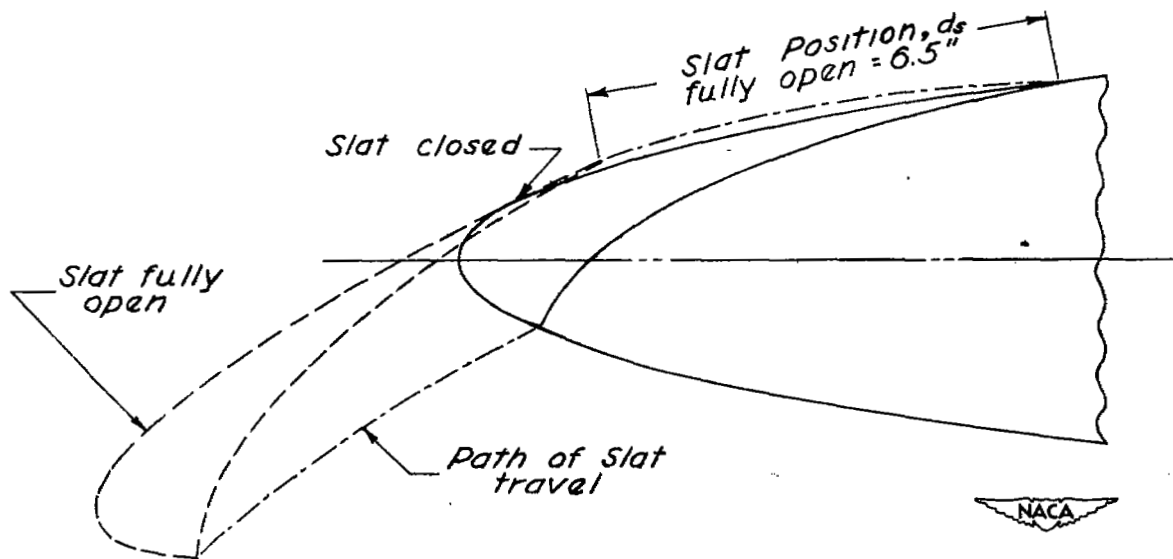


Figure 4.- Section of wing slat of Douglas D-558-II (BuAero No. 37974) research airplane perpendicular to leading edge of wing.

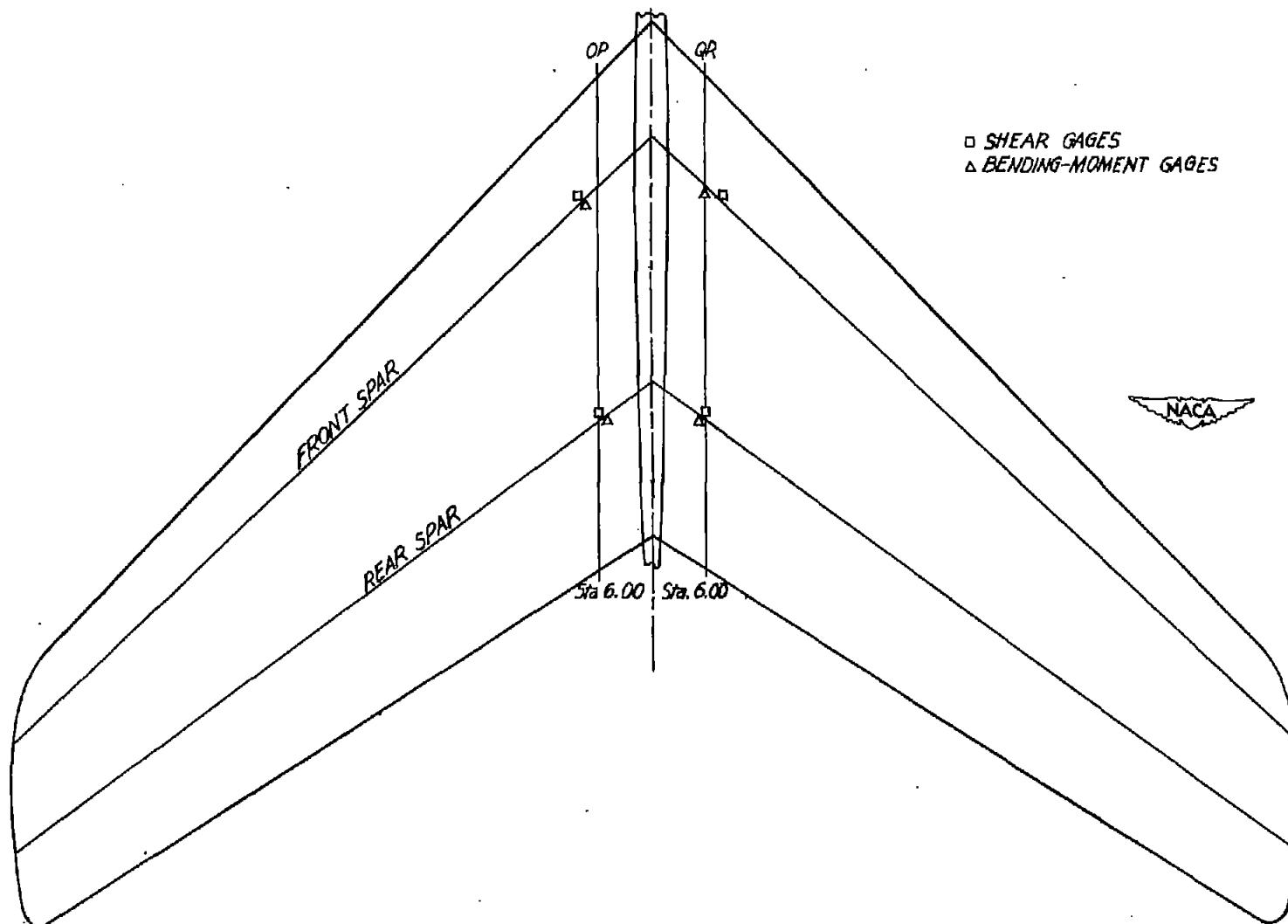


Figure 5.- Locations of strain gages on the horizontal tail of the Douglas D-558-II (BuAero No. 37974) research airplane.

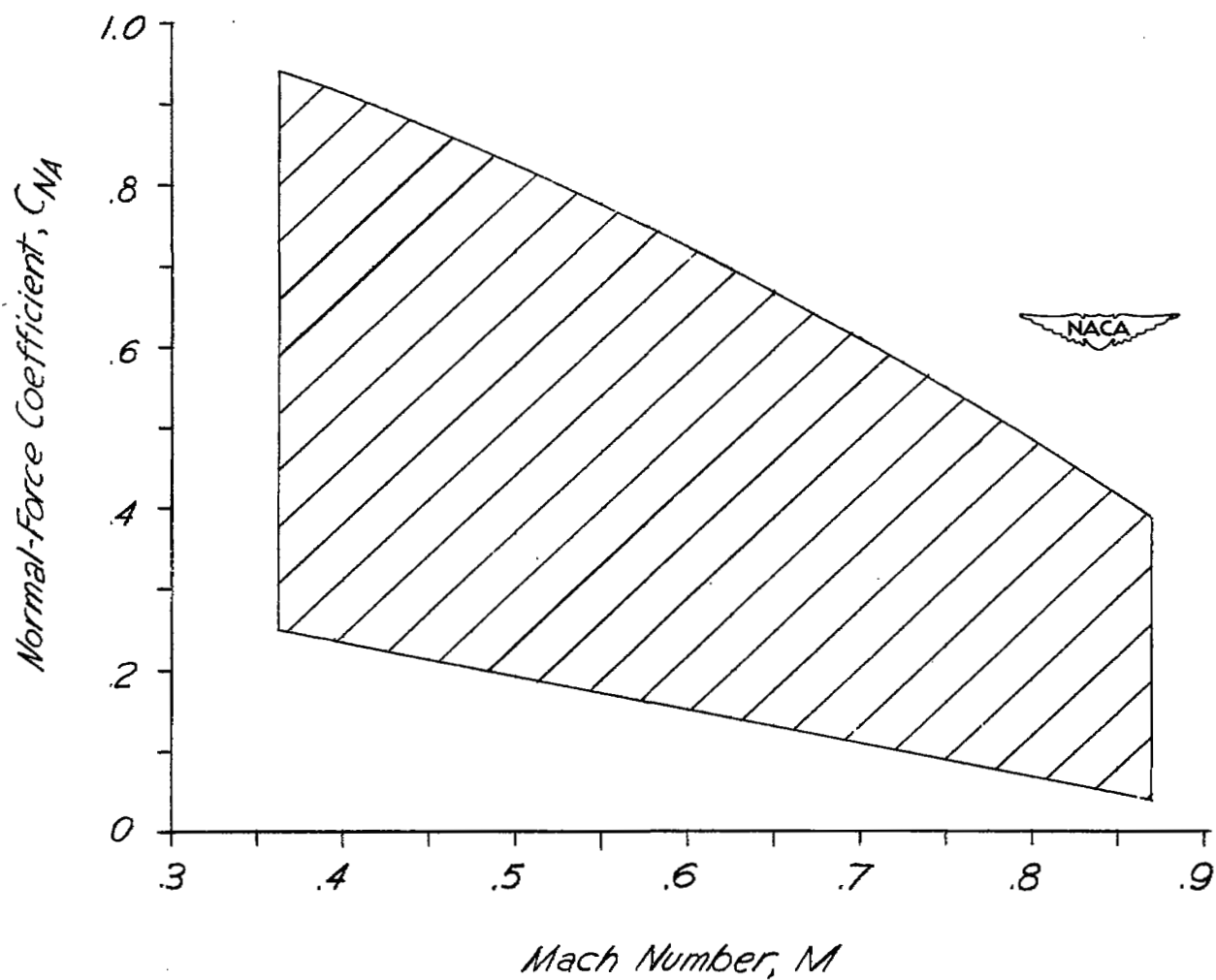


Figure 6.- Range of normal-force coefficients and Mach numbers for which data are presented.

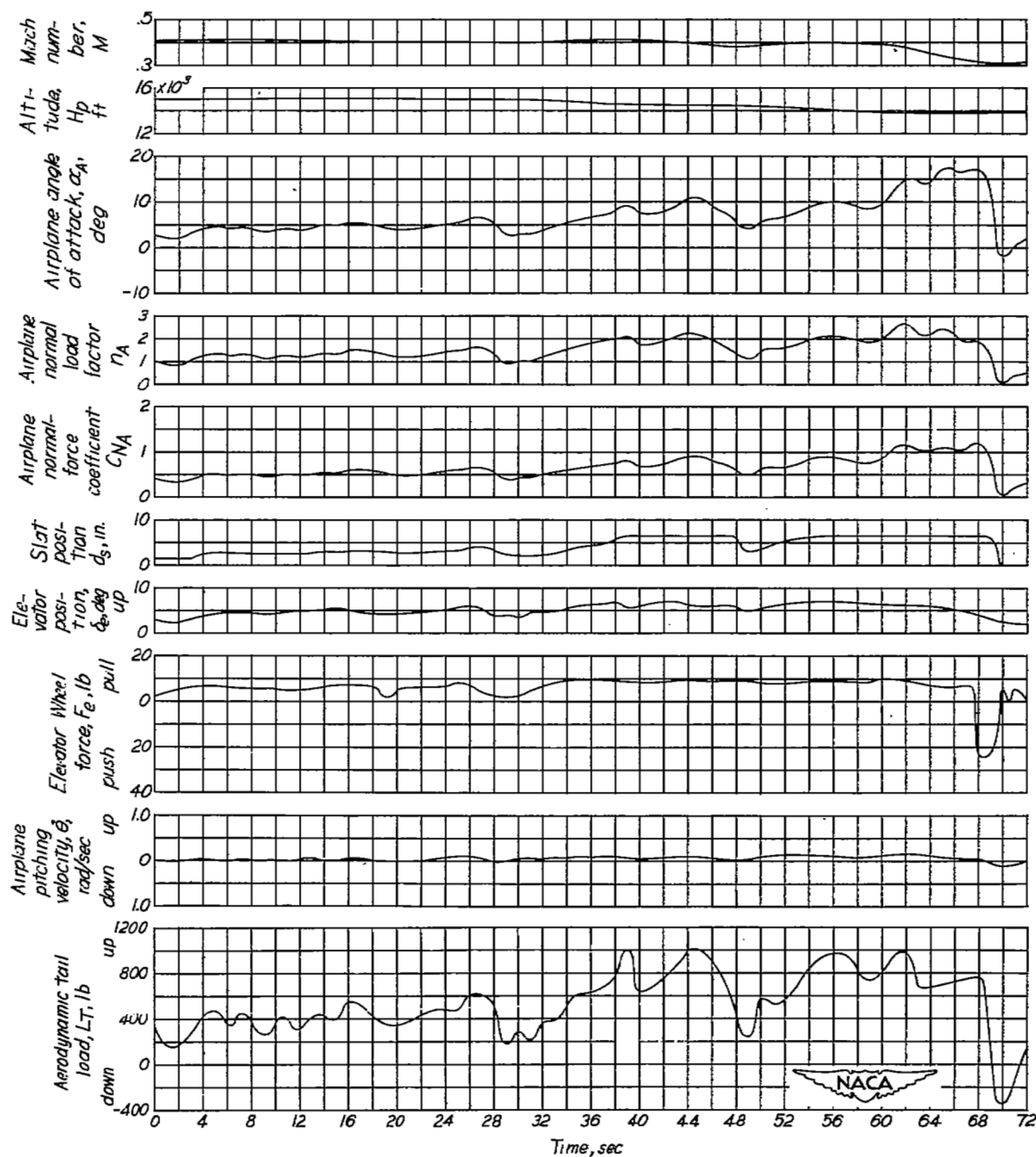


Figure 7.- Time history of a turn with the Douglas D-558-II (BuAero No. 37974) research airplane. Center of gravity at 27.1 percent mean aerodynamic chord; stabilizer setting 1.7° leading edge up.

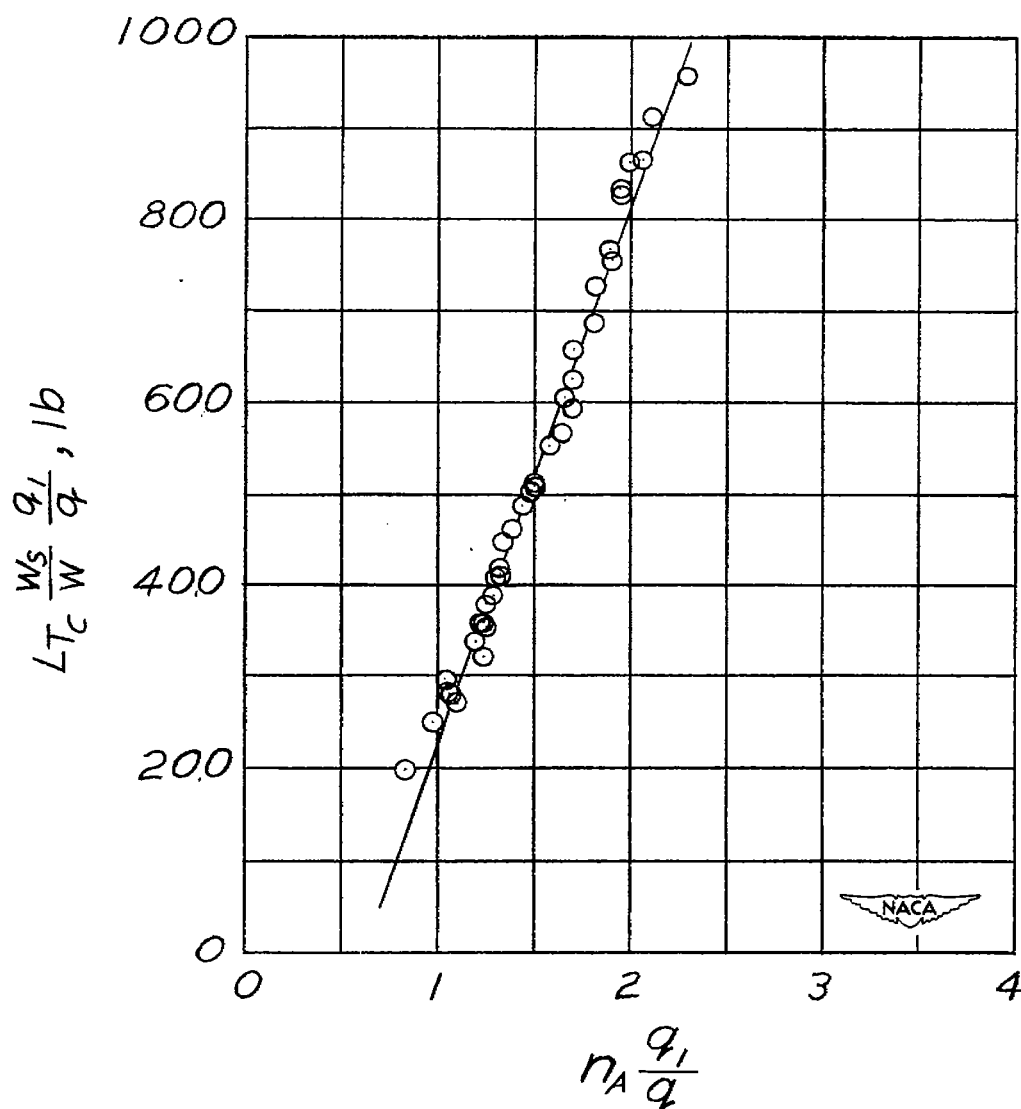


Figure 8.- Variation of corrected aerodynamic horizontal tail load with corrected load factor. W_o , 9600 pounds; q_o , 137.1 pounds per square foot; center of gravity, 27.1 percent mean aerodynamic chord; $\frac{L_F}{c} = 2.73$.

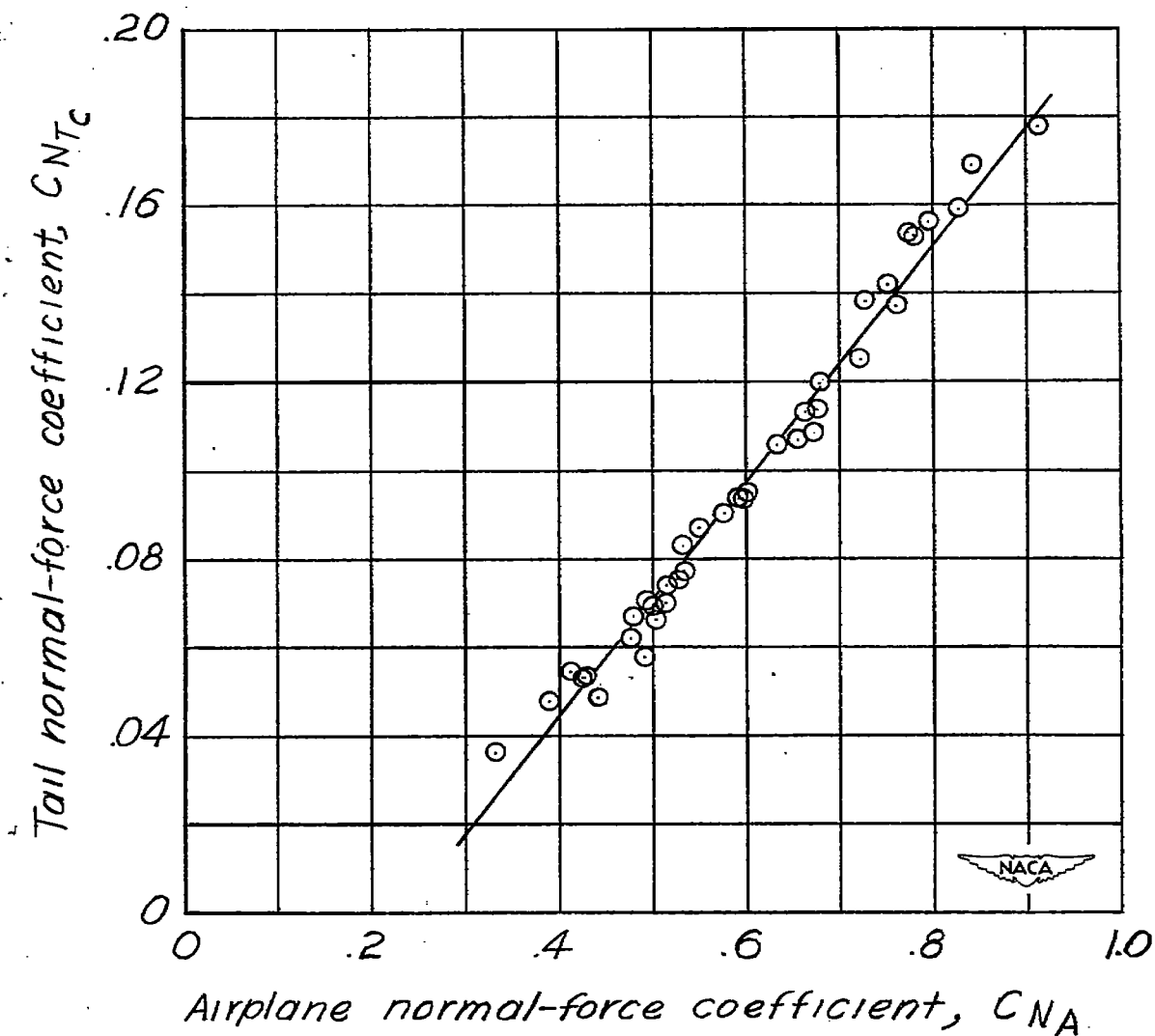


Figure 9.- Variation of horizontal tail normal-force coefficient with airplane normal-force coefficient.

Wing-fuselage aerodynamic center, (a.c.)_{WF}

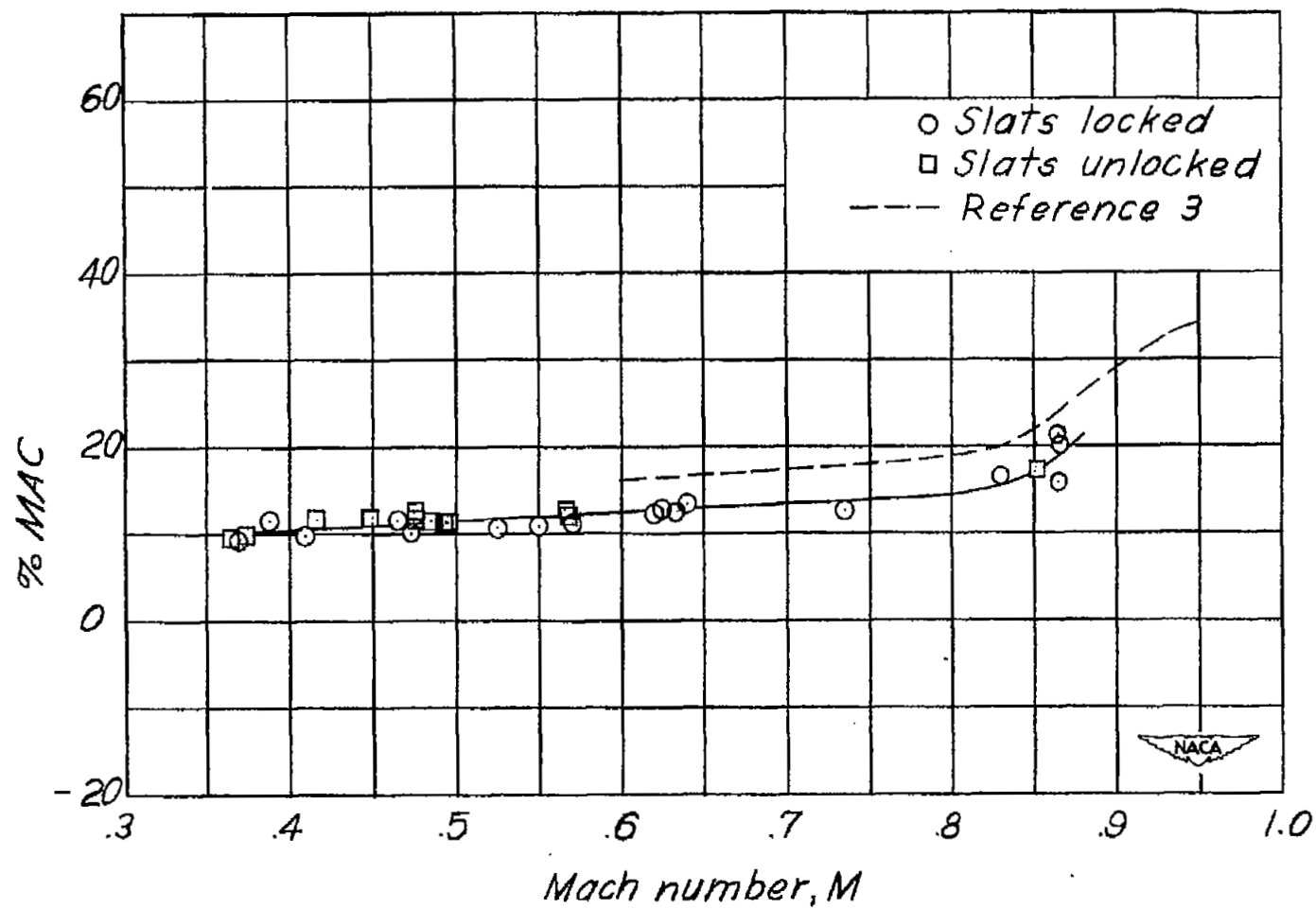


Figure 10.- Variation of the wing-fuselage aerodynamic center with Mach number.

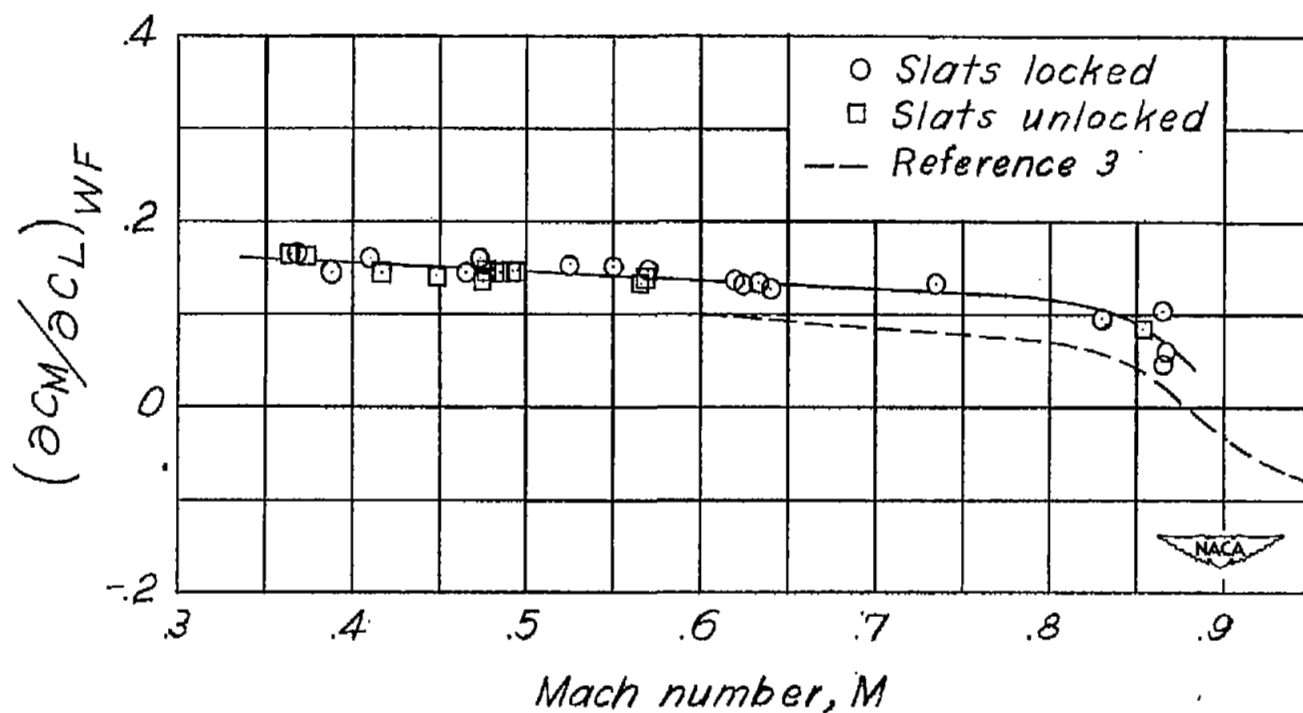


Figure 11.- Variation of the static-longitudinal-stability parameter $(\partial C_M / \partial C_L)_{WF}$ with Mach number. Center of gravity, 26 percent mean aerodynamic chord.

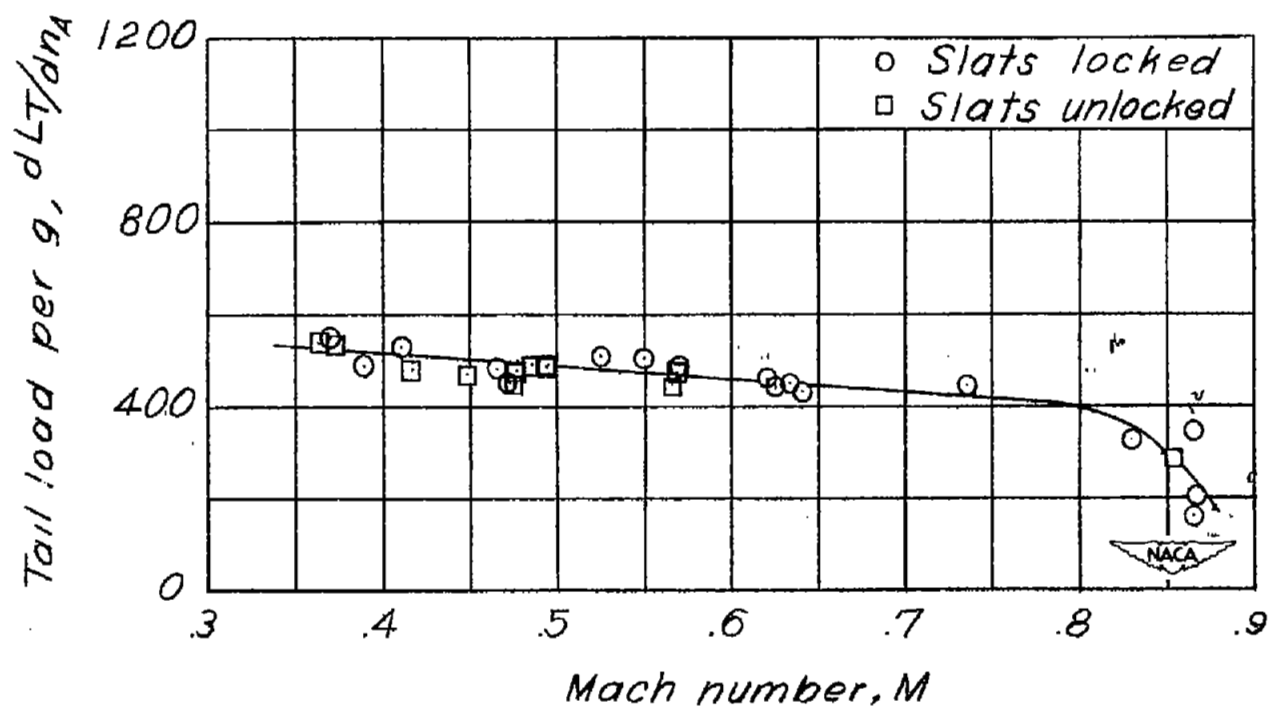


Figure 12.- Variation of the horizontal tail load per g with Mach number.
 W_0 , 9600 pounds; center of gravity, 26 percent mean aerodynamic chord.

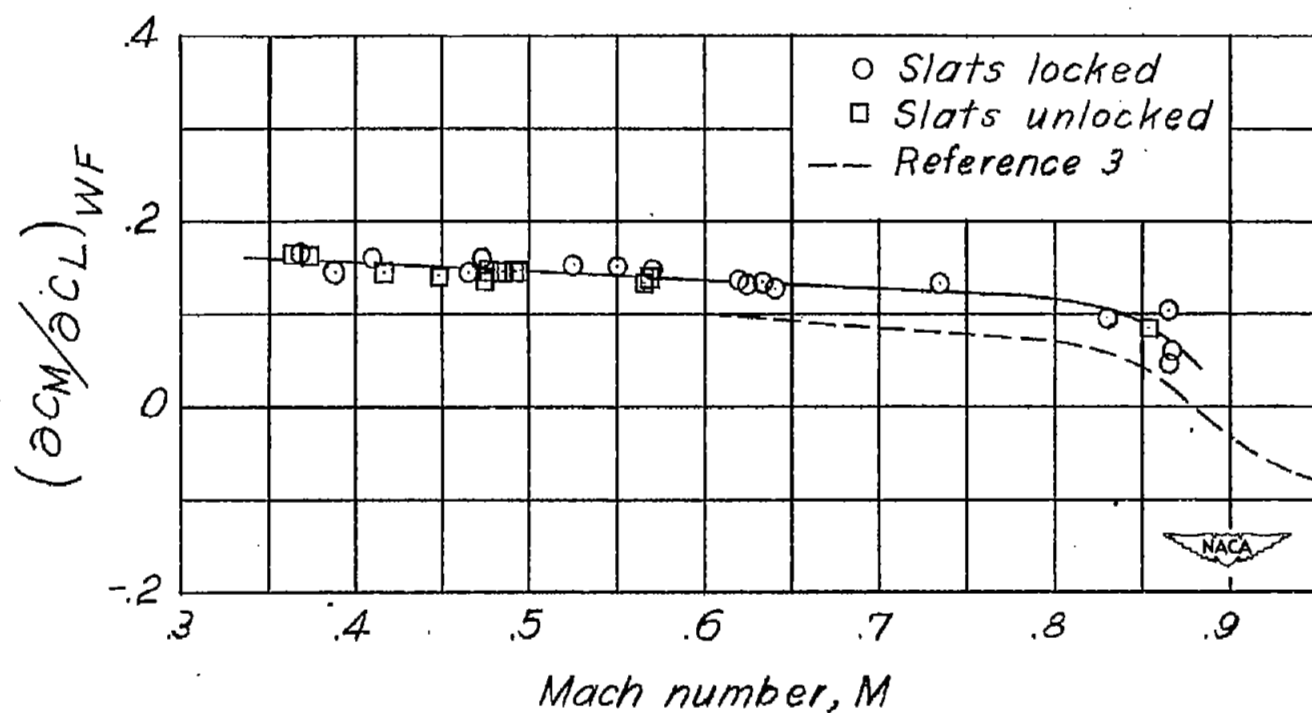


Figure 11.- Variation of the static-longitudinal-stability parameter $(\partial C_M / \partial C_L)_{WF}$ with Mach number. Center of gravity, 26 percent mean aerodynamic chord.

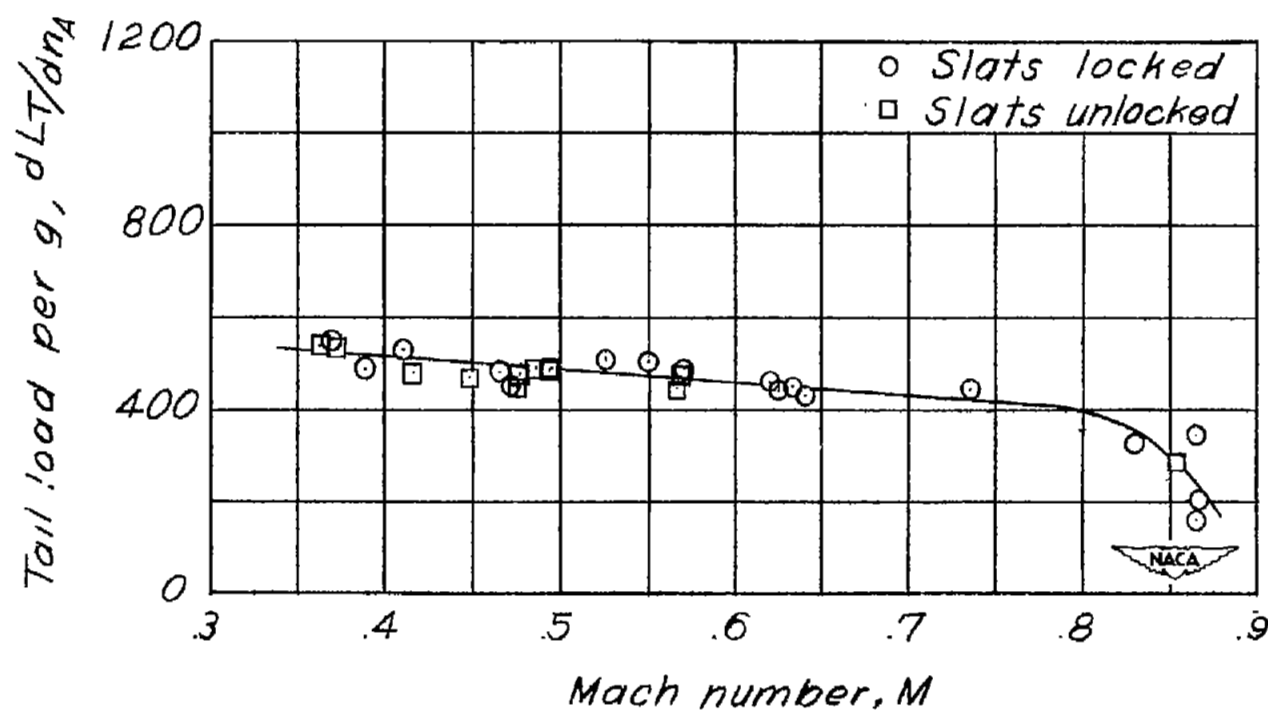


Figure 12.- Variation of the horizontal tail load per g with Mach number.
 W_0 , 9600 pounds; center of gravity, 26 percent mean aerodynamic chord.

Zero-lift wing-fuselage
pitching-moment
coefficient, $(C_{M_0})_{WF}$

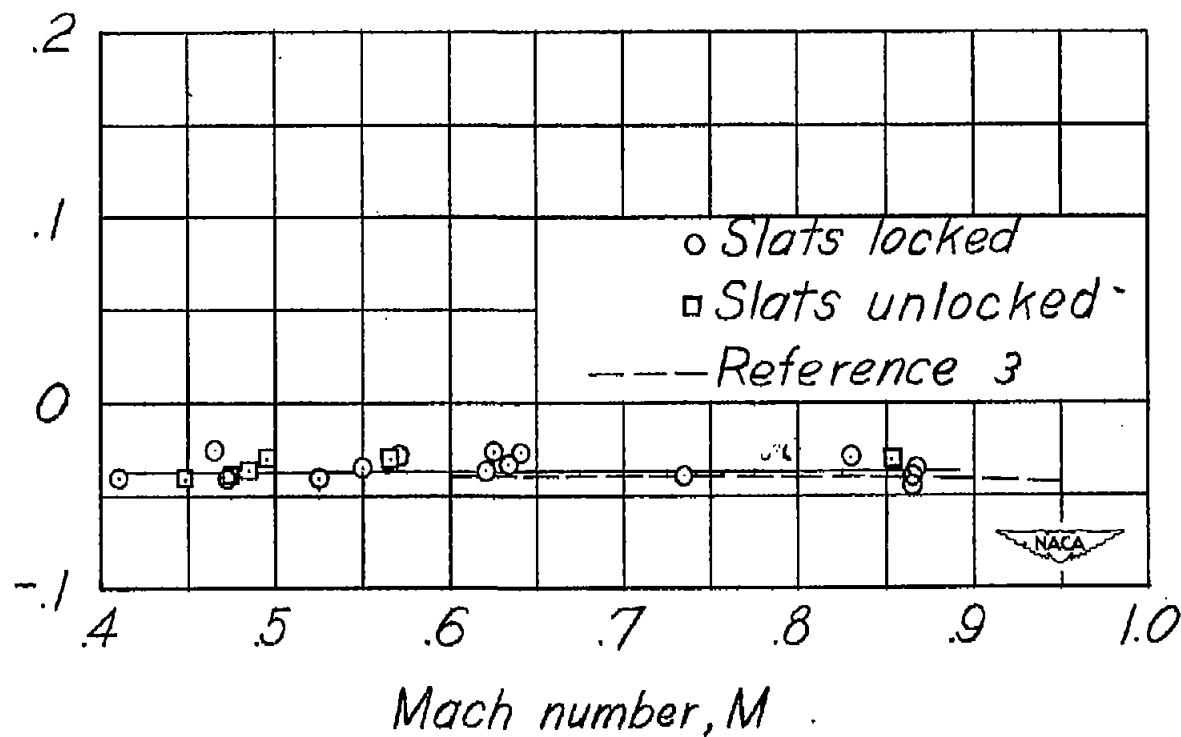


Figure 13.- Variation of the zero-lift wing-fuselage pitching-moment coefficient with Mach number.

NASA Technical Library



3 1176 01437 0416